Proceedings 10th NUMGE 2023
10th European Conference on Numerical Methods in Geotechnical Engineering
Zdravkovic L, Kontoe S, Taborda DMG, Tsiampousi A (eds)

https://doi.org/10.53243/NUMGE2023-96

Mesoscale FEM approach on cemented sand: challenges and implementation of high order elements

M. Komodromos[1], M. Gorji[2], A. Düster[2], J. Grabe[1]

[1]*Institute of Geotechnical Engineering and Construction Management, Hamburg University of Technology, Hamburg, Germany*

[2]*Institute for Ship Structural Design and Analysis, Hamburg University of Technology, Hamburg, Germany*

ABSTRACT: The rapid development of 3D imaging techniques, combined with image analysis, has enabled the quantification of the morphology of multiphase media. One step beyond, the ability to mesh the captured geometry allows the numerical testing of the digital twin, proven to be a valuable numerical tool in material investigation and micro-macro implementations. The scope of this study is the implementation of a finite element discretization of 3D images of cemented sand. The proposed method of the image adapted meshing technique has been implemented and linked to the FE framework of the commercial code ABAQUS Standard. The evaluation of the results demonstrates both accuracy and efficiency in capturing the causes that trigger matrix cracking and grain crushing. Furthermore, computational challenges of excessive stiffness and parasitic stresses are addressed and solved by increasing the order of the elements used. This attempt required the development of an add-on feature to the Delaunay triangulation algorithm, which enriches constant strain tetrahedral elements with nodes at the midpoints of their edges and upgrades their shape functions from linear to quadratic.

Keywords: cemented sand; X-ray CT; mesoscale FEA; high order tetrahedral elements;

1 INTRODUCTION

The investigation of the micromechanics of cemented granular material is a demanding task, calling for methods capable of capturing the interaction of the incorporated particles and the binding matrix. In the case of dry, coarse granular material, the Discrete Element Method (Cundall, 1979) is one of the dominant numerical tools, thanks to its capacity of handling the intergranular interaction via the implementation of rigid body motion and contact laws in the prediction of the response of the particle assembly under applied loading. In addition, multiple numerical works on the simulation of cemented granular material have been realized using

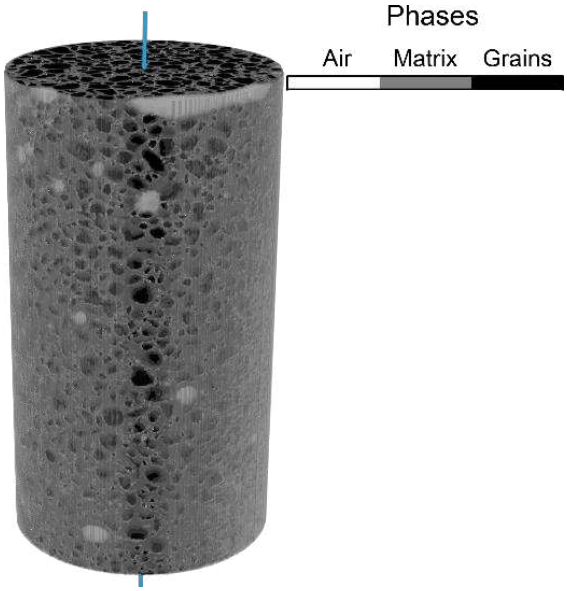

Figure 1. X-ray CT reconstructed 3D volume

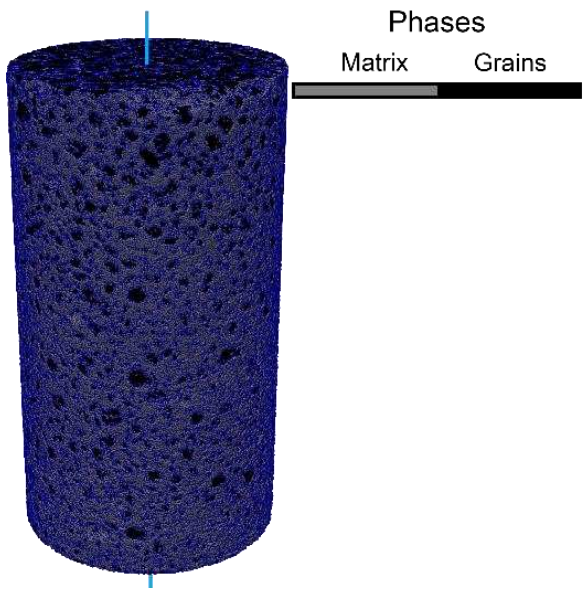

Figure 2. Tetrahedral 3D equivalent mesh

bonding between the incorporated particles (Nguyen, 2022; de Bono, 2014).

Nevertheless, in cases of highly cemented granular material, the irreversible motion of grains, which macroscopically is addressed as *plasticity*, is restrained by the binding mortar and the load bearing mechanism is shifted to the stress transmission along the binder, rather than the direct interplay between the incorporated particles. Against the challenge of predicting the stress distribution through the composite, the Finite Element Method presents some significant benefits. Thanks to its Lagrangian mesh based formulation (Zienkiewicz, 2014), it is able to the capture and predict accurately developing stress conditions in small deformations. Furthermore, image-based meshing techniques are able to sufficiently approximate and pass the morphological information of the scanned composites to the meshed computational domain (Figures 1 and 2), which is later assigned boundaries and solved. Apart from the precise morphological information on the internal structure of the cemented granular material, the discretized domain requires accurate computational modalities in order to reproduce sufficiently the stress localization developing at the mesoscale.

2 MESOSCALE FINITE ELEMENT ANALYSIS

As claimed by scientific studies and available published literature, the complex behaviour of geomaterials is widely addressed to emerge from the shapes of the grains and arrangement of the granular assembly (Calvetti, 1997; Wiebicke, 2017) that form a quite complex fabric of contacts which enables the transmission of loading. The addition of the cement phase appends another morphological crucial parameter, which is the spatial distribution of the binder along the available pore space. The precise quantification of this crucial morphological information has been made feasible by the breakthrough development of the X-ray scanning modalities (Desrues, 2010), which capture and express it in the form of 3D reconstructed image volumes (Figure 3). The correction of beam hardening bias and shining artefacts on these domains via image analysis filters (Figure 4) enables their trustworthy segmentation (Figure 5), resulting into phase distinguished volumes of the constituent materials. In the current study, the communication between the phase morphology in images and the FE solver of Abaqus Standard has been achieved via the image adapted meshing technique, as formulated by calling functions of the powerful meshing library CGAL (CGAL, 2022).

The creation of an equivalent discretized domain based on 3D images (Figure 6) is described by the following principles, considerably divergent from the CAD-CAE bridging which is used in generic structural FE simulations. Initially, the topological information that corresponds to the material interfaces and material bulk is extracted from the image. This information forms the 3D boundary representation of the individual components of the multiphase cemented sand material. In the next step, points are generated on the formed domains, based on maximum discretization distances along the bulk and the interfaces that will serve as future interface and bulk nodes. These point databases are introduced to Delaunay triangulation functions that generate four-node tetrahedral solid elements (commonly referred as *tet4*) and three-node triangular interface elements (commonly referred as *tri3*). Finally, one last communication protocol between the formed mesh and the reference segmented image enables the sorting of elements in sets, according to the materials that they topologically correspond to.

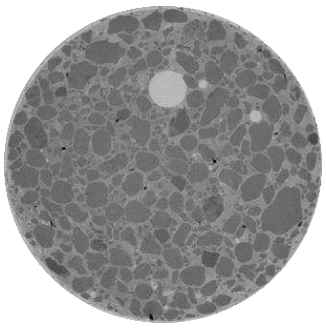

Figure 3. Raw image

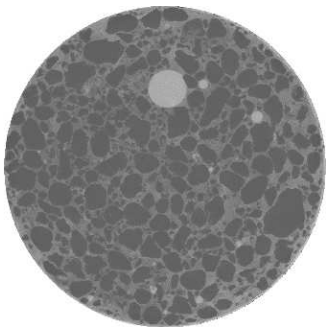

Figure 4. Corrected image

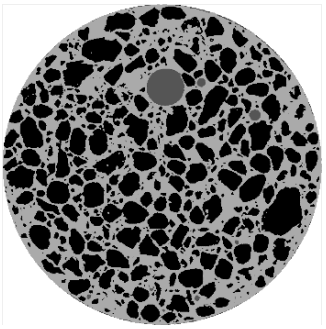

Figure 5. Segmented image

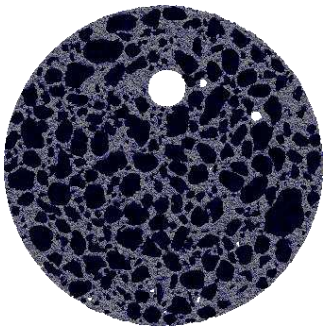

Figure 6. Meshed image

A simple parametric study was performed to inspect the capacity of the meshing algorithm to transfer the morphological information to the mesh. The maximum triangulation distance on the bulk (*bulk dist*) was altered and the maximum triangulation distance at the interfaces (*interf dist*) was kept constant to the essential value of one voxel. The agreement between the reference image and the generated meshes was quantified by drawing label plotlines along the central axial path of the domain, as indicated by the blue vertical line in Figures 1, 2. Indeed, a sufficient match between the reference image and the mesh is quantitatively confirmed by the label plotline and visually displayed by the mesh rendering (Figure 7), under the condition of small

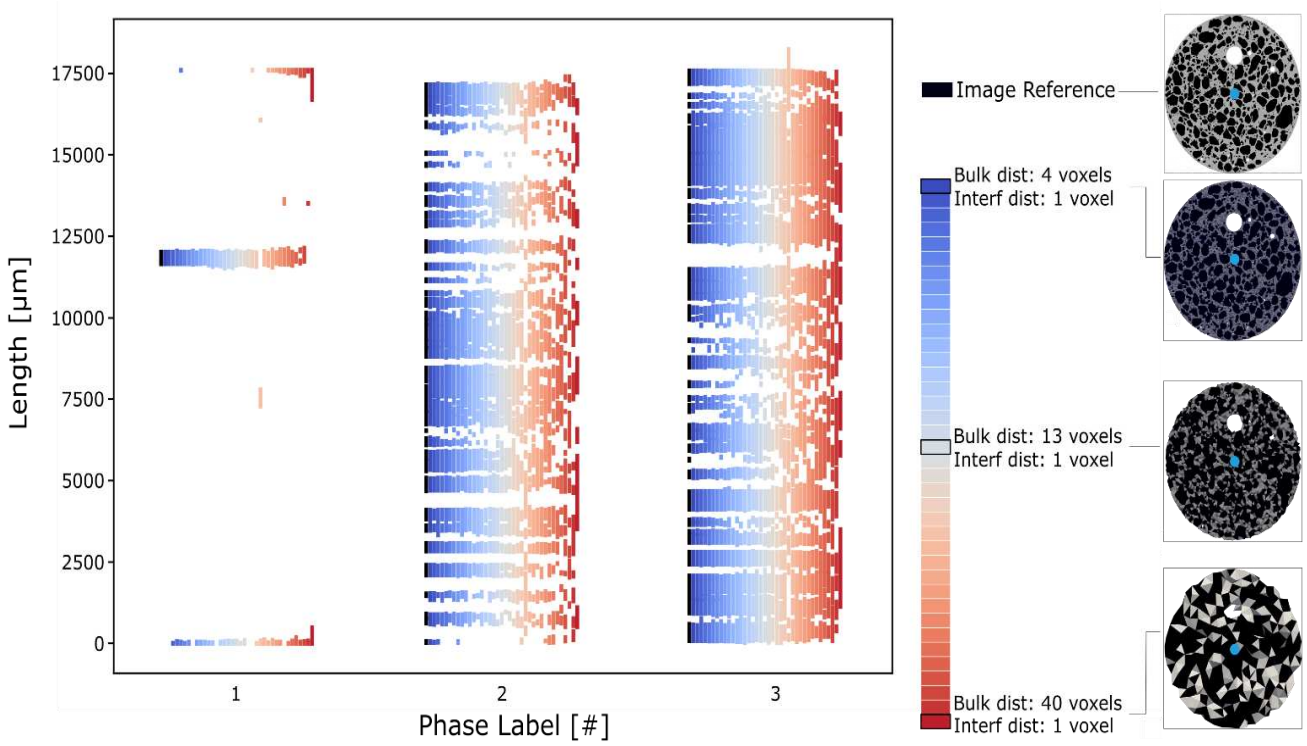

Figure 7. Morphological reproducibility study

magnitudes of the bulk discretization distances. Still, the trade-off between precise morphological reproducibility and computational efficiency needs to be considered, therefore the study has been limited to meshes that consist of less than 7.1 million nodes.

3 PRECISION UPGRADE VIA SECOND ORDER TETRAHEDRA ELEMENTS

The translation of the imaged morphology of natural sand particles, cement mortar and macro pores into a discretized domain has been realised by the use of tetrahedra and triangles. These geometric entities are chosen for the discretization of demanding geometries, thanks to their capacity of effectively approximating the volume and surface of any arbitrary shape given (Bukenberger, 2021). In order to keep the model simple, the interface elements were removed, establishing fixed interfaces between the grains and the coating cement mortar. In addition, the macro pores were explicitly excluded from the meshing process in favour of numerical stability and efficiency.

Nevertheless, the use of four-node tetrahedra is a controversial matter in FEA (Zienkiewicz, 2014). Despite of their performance in approximation of complex shapes, the accuracy of four-nodes tetrahedra may present significant issues to the final result output. Specifically, the assigned linear shape functions, which are formulated on the standard four nodes and a single integration point placed at the centroid of the element, allow the tetrahedron to deform in a linear manner, causing a number of numerical parasitic phenomena and questioning their ability to capture the mechanical behavior. In standard CAD-CAE simulations, the ordinary evidence of element dysfunction is excessive stiffness and moderated deformation (Choi, 2018), which calls for finer discretization, until the point when the simulation becomes mesh independent. Another approach of improving the quality of the conducted simulation, apart from brute increase of the elements involved in the simulations, is the elevation of the shape functions of the existing elements from linear to quadratic, altering the elements from constant (Figure 8) to linear strain (Figure 9). Such attempt allows the edges to deform in a quadratic manner, effective countering the aforementioned pathogeneses, by adding six additional nodes at the midpoint of each edge.

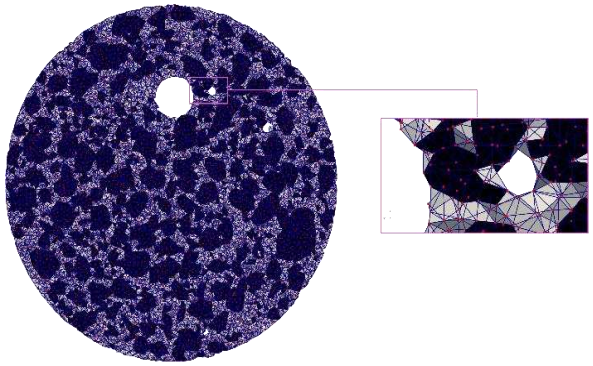

Figure 8. First order mesh

This upgrade was realized by implementing a parallelized expansion to the image adapted meshing engine. In the first step, the required additional nodes are generated at the midpoints of all existing element

edges and their labels are placed at the corresponding position of the connectivity matrix. Then, a search of nodal duplicates is performed, based on the coordinates, which enables a sweeping process of the undesired nodes from the nodal list of the mesh. Finally, the initial nodal labels assigned at the connectivity matrix are corrected via renumbering procedures, ensuring compatibility between all neighbouring elements of the simulation. The sum of nodes for meshes of increasing number of elements shows that this upgrade increases the number of degrees of freedom by the factor of 7 (Figure 10). The current investigation was stopped at a maximum of 6.17 million nodes, corresponding to a maximum bulk discretization distance of 8.5 voxels.

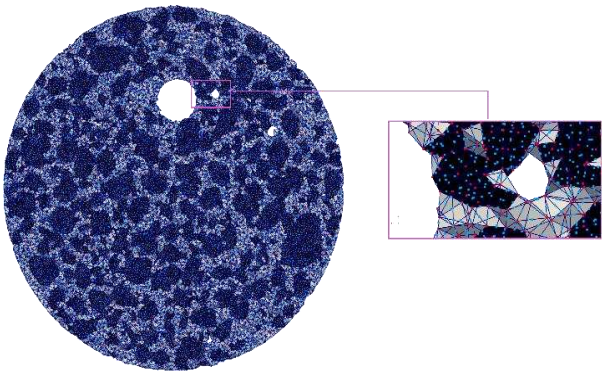

Figure 9. Second order mesh

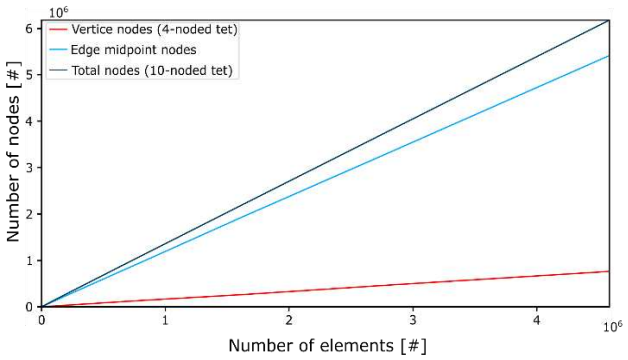

Figure 10. Computational cost of element upgrade

4 MICROMECHANICS DISPLAY

The direct comparison between the image-based simulations formulated by low and high order tetrahedra is made possible thanks to the implemented element upgrade expansion. An identical uniaxial compression test was applied to both domains, which are defined by a bulk discretization distance of 8.5 voxels, by imposing unit compressive displacement constraint in the axial direction. The computed distribution of the axial displacement along the central plotline of both domains provides a first indication of the advantage in favour of high order elements. Indicatively, quadratic elements present clearer constant displacement trends at the positions of the grains and steeper displacement tendency at the positions in-between (Figure 11), thus deal better with the standard granular mechanics which propose rigid body motion for the quasi rigid particles. The linear tetrahedral elements are able to merely capture a similar pattern of these mechanisms. Nevertheless, the output of low order is quite blurrier due to numerical inaccuracy, which does not allow the capture of sudden jumps and discontinuities in the kinematic field.

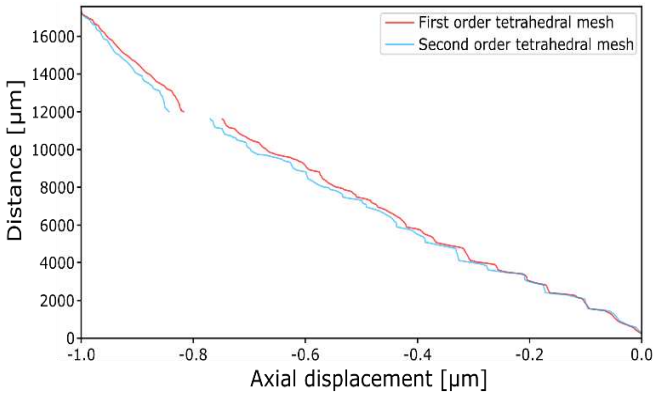

Figure 11. Axial displacement along the central plotline

The superiority of quadratic elements is plainly confirmed by contours of the von Mises equivalent stress distribution, which expresses the deviatoric state at each position of the domain. Linear strain tetrahedra are able to capture precisely the stress development at the *very close range* of the particle edges, which is expected by the high stiffness contrast between the Quartz particles and the diluted cement mortar. In addition, the high stress at the intergranular contacts is *localized* at the contact points, presenting peak magnitudes (Figures 12 and 13). On the other hand, constant strain tetrahedra are able to merely capture these phenomena, but lack in their accurate quantification. Indicatively, the stress is not localized on the expected positions of contacts and granular edges. Instead, it presents moderate values and is propagated to the greater neighbouring volumes (Figures 12 and 14), which should not actively contribute at the sustaining of the load. This last statement can be confirmed by having a close look at the regions around the macro pores. While the high order elements clearly display the zero stresses around the voids (free surface boundary), low order elements display parasitic large

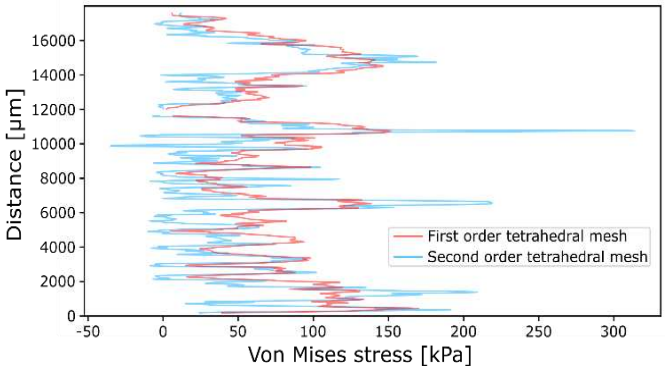

Figure 12. Von Mises stress projection on central plotline

magnitudes close to that boundary. This misfunction, apart from displaying a blurry output of the unfolding mechanisms, could also lead to errors in non-linear analyses predicting matrix cracking and particle breakage, two mesoscale phenomena triggered by the stress localization, whose blend forms the macroscopic failure of cemented sands (Tengattini, 2014; Das, 2014).

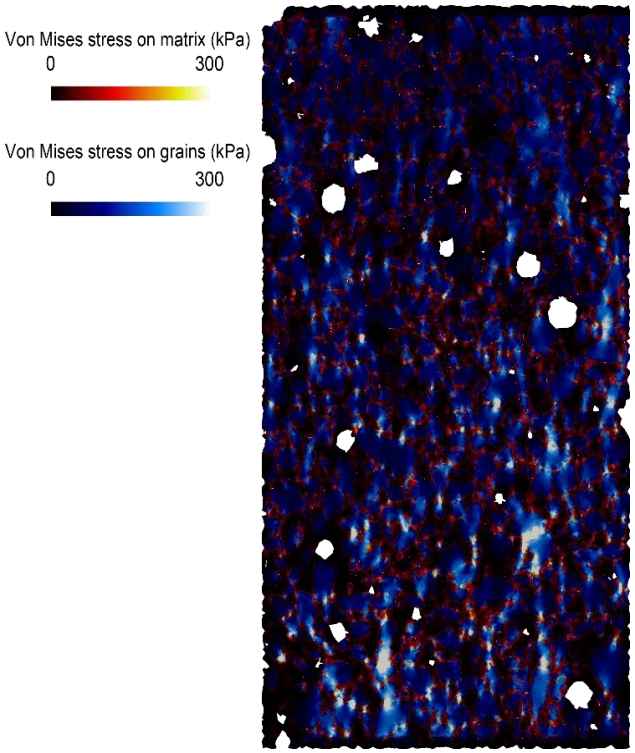

Figure 13. Von Mises stress display (quadratic elements)

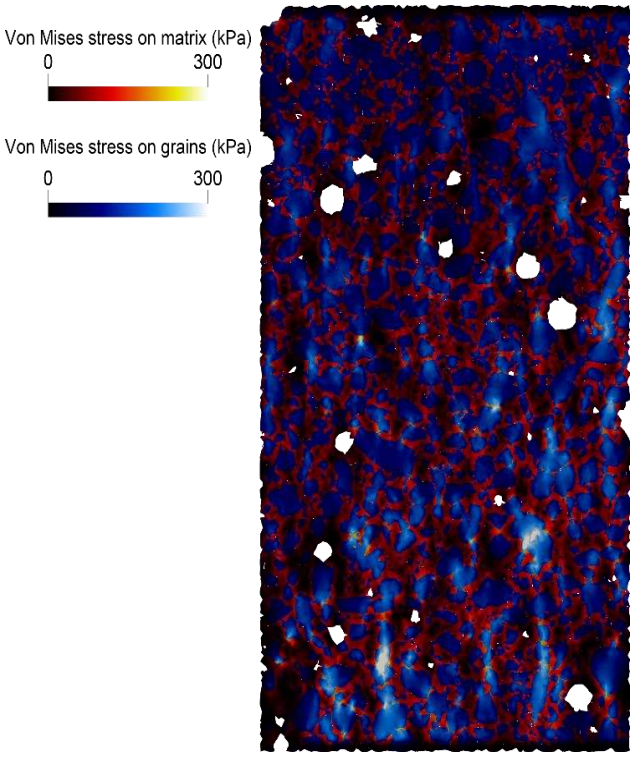

Figure 14. Von Mises display (linear elements)

5 CONCLUSIONS

This work addressed the challenges of the FEM practice in the investigation of cemented granular material at the mesoscale and provided solid evidence on its capacity of capturing the load sustaining mechanisms that unfold through the volume of the composite. The fact that the binding substance suppresses granular movement and renders brittle behavior, which does not exceed small strains, makes the FE simulation feasible and efficient. Moreover, the consideration that the matrix controls the stress transmission provides solid conditions for the continuum based framework of the FEM. This is not the case in dry granular material, where large deformations and the incorporation of multiple bodies demands the transition to particle based methods, such as the DEM. Concerning the reliability of the simulation, two main parameters are addressed and examined. The first one is clearly geometrical and concerns the matter of similarity between the imaged volume and the produced mesh, which can be improved by increasing the nodal density in the discretization process. The second one is purely numerical and considers the ability of the implemented elements to handle the demanding stress states associated with the high contrast in stiffness and the touching points between the grains. According to a direct comparison between simulations of linear and quadratic elements, it is shown that patterns of stress localization are emerging and their capture is made possible under the condition of high precision, which is satisfied by quadratic tetrahedra. In the case of low order elements, the stress concentration is still identified, but there is a clear weakness in localization prediction, which could cause serious error in fracture prediction, occuring either as matrix cracking or particle breakage. Since the image based simulations fundamentals are impoved and evaluated, the next step of investigation is advancement on numerical modelling, incorporating the eXtended Finite Element Method (XFEM) (Belytschko, 1999; Moës, 1999), incorporated under the approach of Linear Elastic Fracture Mechanics (LEFM) (Griffith, 1921; Irwin, 1958; Rice, 1968).

6 ACKNOWLEDGEMENTS

The authors gratefully acknowledge the financial support support provided by the DFG (Deutsche Forschungsgemeinschaft) under the grant number GR 1024/41-1 and DU 405/17-1 and the beam time provided by Laboratoire 3SR, Grenoble, France.

7 REFERENCES

Belytschko, T., Black, T. 1999. Elastic Crack Growth In Finite Elements. *International Journal for Numerical Methods in Engineering,* **45**, 601-620.

Bukenberger, D. R. and Lensch, H. P. A. 2021. Tetrahedra of varying density and their applications. *The Visual Computer,* **37**, 2447–2460.

Calvetti, F., Combe, G. 1997. Experimental micromechanical analysis of a 2D granular material: relation between structure evolution and loading path. *Mechanics of Cohesive-Frictional Materials,* **2**, 131-163.

CGAL, 2022. *CGAL User and Reference Manual.* s.l.:CGAL Editorial Board.

Choi, J. H., Lee, B. 2018. Development of a 4-node hybrid stress tetrahedral element. *International Journal for Numerical Methods in Engineering,* **113**, 1711-1728.

Cundall, P. A., Strack O. D. L., 1979. A discrete numerical model for granular assemblies. *Géotechnique,* **29***,* 47-65.

Das, A., Tengattini, A., Viggiani, G., Nguyen, G. 2014. A thermomechanical constitutive model for cemented granular materials with quantifiable internal variables. Part II - Validation and localization analysis. *Journal of the Mechanics and Physics of Solids,* ***70***, 382-405.

de Bono, J. P., McDowell G. R., Wanatowski, D. 2014. DEM of triaxial tests on crushable cemented sand. *Granular Matter,* **16**, 563–572.

Desrues, J., Viggiani, G., Besuelle, P. 2010. *Advances in X-ray Tomography for Geomaterials,* Wiley, New York.

Griffith, A. 1921. The phenomena of rupture and flow in solids*. Philosophical Transactions of the Royal Society of London. Series A, Containing Papers of a Mathematical or Physical Character*, **221,** 163-198.

Henderson, A., 2007. *ParaView Guide, A Parallel Visualization Application.* Kitware Inc.

Irwin, G.R., 1958. *Fracture, Elasticity and Plasticity,* Springer, Berlin.

Moës N., Dolbow, J., Belytschko, T. 1999. A finite elemet method for crack growth without remeshing, *International Journal for Numerical Method in Engineering,* **46**, 131-150.

Nguyen, T., Desrues. J., Vo, T. T., Combe, G. 2022. FEM×DEM multi-scale model for cemented granular materials: Inter- and intra-granular cracking induced strain localisation. *International Journal for Numerical and Analytical Methods in Geomechanics,* **46**, 1001– 1025.

Rice, J., 1968. *Fracture, an Advance Treatise.* Academic Press, Cambridge, Massachusetts.

Smith, M. 2009. *ABAQUS/Standard User's Manual, Version 6.9.* Providence, Dassault Systèmes Simulia Corp,.

Tengattini, A., Das A., Nguyen, G. D., Viggiani., G., Hall, S. A., Einav, I. 2014. A thermomechanical constitutive model for cemented granular materials with quantifiable internal variables. Part I-Theory. *Journal of the Mechanics and Physics of Solids,* **70**, 281-296.

Wiebicke, M., Andò, E., Herle, I., Viggiani G. 2017. On the metrology of interparticle contacts in sand from x-ray tomography images. *Measurement Science and Technology,* **28**.

Zienkiewicz, O.C., Taylor, R.L., Fox, D., 2014. *The Finite Element Method for Solid and Structural Mechanics.* Butterworth-Heinemann, Oxford.